X-ray radiation measurement from electrons accelerated in low-density plasma Petawatt laser interaction

S. Kneip, S. R. Nagel, S. P. D. Mangles, L. Willingale, P. M. Nilson, A. E. Dangor, Z. Najmudin and K. Krushelnick
The Blackett Laboratory, Imperial College London, Prince Consort Road, London, SW7 2BW, UK

K. Ta Phuoc, N. Bourgeois, A. Rousse and J. R. Marquès
Laboratoire d'Optique Appliquée, ENSTA, CNRS UMR7638, Ecole Politechnique, Chemin de la Hunière, 91761 Palaiseau, France

Main contact email address stefan.kneip@imperial.ac.uk

Introduction

Electrons accelerated in electric fields give rise to emission of characteristic electromagnetic radiation, which, when measured, may allow to infer electron acceleration dynamics thus contributing to the understanding of the field of laser particle acceleration.[1,2] We report on the first efforts to field x-ray diagnostics, including knife edges, Ross filter pairs, a pinhole camera and a crystal spectrometer on Petawatt laser interactions with underdense plasmas formed from the ionization of a helium gas jet. At focused intensities of $>2 \times 10^{20}$ Wcm^{-2} electrons can be accelerated in cavitated channels to energies in excess of 300 MeV, travelling with highly nonlinear trajectories which will give rise to x-ray radiation.[3] The idea of this experimental campaign was to assess the usability of the aforementioned x-ray diagnostics on a typical low repetition rate gas jet experiment on a Petawatt laser. The goal is to fully characterize the angular and spectral x-ray emission pattern as well as the emission source size and consequently determine the dynamics of the energetic electrons.

Experimental Setup

The experiments were performed using the Vulcan Petawatt laser. The laser pulse had a duration of (0.49±0.08) ps and an energy up to 360 J on target with a central wavelength of 1.055 µm. An *f/3* off axis parabolic mirror focused the laser onto the front edge of a gas jet, which had a 2 mm supersonic brass nozzle with a 5×6 µm^2 FWHM focal spot size in vacuum. This corresponds to a w_0=3.3 µm Gaussian beam waist compared to a diffraction limited waist of $w_0=\lambda F^{\#}$=3.2 µm.[4] For some shots, the 2 mm brass nozzle was replaced by a 5 mm plastic nozzle. In addition to that, the Rayleigh range of the focal spot could be changed from 30 µm to 84 µm by apodizing the beam from an *f/3* to an *f/5* focusing geometry. This increases the diffraction limited beam waist to w_0=5.3 µm. The averaged focused intensity typically was 2.3×10^{20} Wcm^{-2} and 1.7×10^{21} Wcm^{-2} for an *f/5* and *f/3* shot respectively, yielding normalized vector potentials a_0 of 14 and 37 respectively.

Helium was used as the target gas. The backing pressure could be varied to give electron plasma densities up to 1.4×10^{20} cm^{-3}.

Discussion of Potential Diagnostics

The nature of a low repetition rate Petawatt experiment imposes boundary conditions for the design and setup of any diagnostic to be fielded. Diagnostics have to be run on a single shot basis. Hence, the detection efficiency needs to be high enough to allow for single shot operation. The three most common detection systems for x-ray measurements are scientific x-ray film, x-ray sensitive charge-coupled devices (CCD cameras) and image plates. High sensitivity double emulsion layer x-ray films such as the prominent Kodak DEF have been discontinued some five years ago and are no longer readily available. Less thoroughly characterized industrial x-ray film such as the Kodak Industrex CX film remains as an option. When compared to Fuji Film BAS-MS image plates, available x-ray film has a sensitivity which is about 5 times lower, requiring a minimum number of ~5×10^{-2} photons/µm^2 to produce a measurable signal in a wavelength range from 5.5 to 6.5 Å.[4] An additional benefit of using image plates is that it does not require time consuming chemical processing as necessary for x-ray film. This makes image plate the preferred detector out of the two. CCD cameras have a major advantage over both film and image plates due to their instant readout capability combined with an increase in sensitivity of one to two orders of magnitude.[5] Instant read-out capability becomes less significant on a low repetition rate Petawatt experiment, where turn-around times are on the order of an hour. This leaves sufficient time to cycle the vacuum chamber and replace used image plates by new ones. Furthermore, CCDs require low levels of background radiation. This limits the use of free standing and even flange mounted vacuum compatible chips inside target area Petawatt.

In addition to single shot operation, any diagnostic to be fielded in a Petawatt experiment should have maximum compatibility with other (major) diagnostics, which typically are electron and ion spectrometers as well as optical probing and imaging diagnostics.

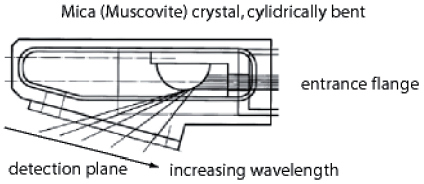

Figure 1. Schematic of defocusing crystal spectrometer.[6]

In order to meet the challenge of characterizing the source spatially and spectrally, the following diagnostics were fielded:

Knife edges and an x-ray pinhole camera provide spatial information of the source. The spectral information obtained with either diagnostic is limited and simply given by the cutoff energy of the filter used. Penumbral imaging

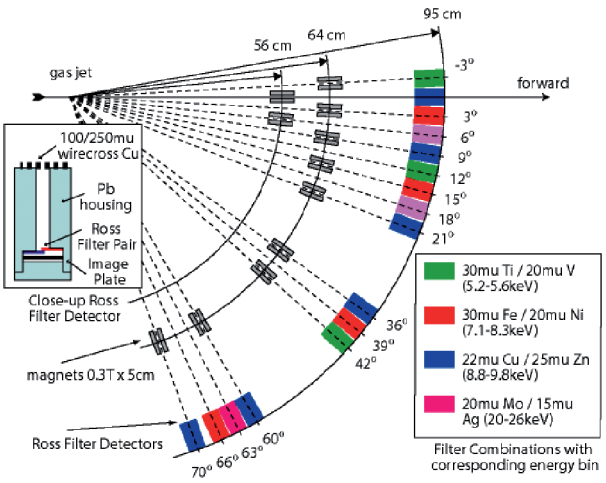

Figure 2. Schematic setup of Ross filter detectors. An array of Ross filter pairs is set up in a radial configuration spanning angles from -3° to 70° from the forward direction. The top left inset is a close up showing the design of a Ross filter pair assembly.

by means of a knife-edge yields 1D spatial information, is easy to set up and can be run in parallel to charged particle spectrometers. Pinhole imaging yields fully 2D spatial information but may require more time to set up and a few iterations to optimize the magnification and field of view. Ideally, magnets should be used to deflect background electrons. However such magnets were found to conflict with the electron spectrometer which was operated in parallel.

A commercially available x-ray spectrometer based on a defocusing crystal made from mica was used in *(hkl)=(004)* reflection (2nd order, *2d=9.92 Å*) (Fig.1). This configuration can access a wide spectral window from 3 to 10 Å and requires much less rigorous alignment than spectrometers based on focusing crystals. When attached to a flange behind the electron spectrometer with a direct line of sight to the target, the x-ray flux entering the spectrometer was found to be too small to produce a spectrum. When placed inside the chamber, fluorescence from the crystal caused by the ubiquitous electron background dominates over the signal, even though magnets and lead shielding were implemented.

An alternative way to obtain spectral information is the Ross filter method. It is based on a pair of metal foils of similar atomic number. The thickness of the foils is chosen to match the x-ray attenuation characteristics over the whole spectrum except for the energy bin given by the slightly different K-alpha absorption edges. Therefore the relative difference of the transmitted signal can be attributed to this energy bin. Its advantages over crystal spectrometers are a considerably smaller loss of intensity and the absence of harmonics or overlapping orders.

To obtain angular and spectral resolution, an array of Ross filter pairs was set up in a radial configuration (Fig. 2). Various filter combinations of suitable thickness have been chosen carefully to build Ross filter pairs with energy bins 5.2-5.6 keV, 7.1-8.3 keV, 8.8 to 9.8 keV and 20-26 keV as depicted on the inset of Fig 2.

Results

For the first series of shots, a pinhole camera and a knife edge were fielded. The pinhole camera was set up in forward direction, at 26°±3° out of the horizontal plane to leave a clear line of sight to the electron spectrometer. The distance from the pinhole to the front edge of the nozzle was 6 cm, the distance from the pinhole to the imaging plate was 28 cm, yielding a magnification of 4.7 and a field of view of 8 mm diameter. The 50 µm diameter pinhole was covered with a 20 µm Mg foil which has a *1/e* cutoff energy of 4 keV. Fig. 3 shows an image of the x-ray source for a plasma density of 1.4×10^{20} cm^{-3} and averaged focused intensity of 1.2×10^{21} Wcm^{-2}. Lineouts in horizontal and vertical direction yield a FWHM source size of (1.2±0.2) mm and (0.7±0.2) mm respectively. It can be seen clearly that the source is much further extended in the horizontal direction than it is in the vertical direction.

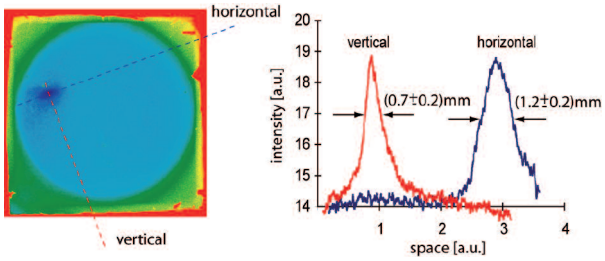

Figure 3. (left) Focal spot image taken with an x-ray pinhole camera filtered with 20 µm Mg foil with *1/e* cutoff energy 4 keV. (right) Horizontal and vertical lineouts yield source size.

In parallel to the pinhole camera, the two orthogonal blades of a knife edge were inserted in the forward direction, 12 cm from the target and 114 cm from the imaging plate yielding a magnification of 9.5. The three images in Figure 4 show the shadow caused by the razor blade in the bottom left corner. The intensity variation along a lineout across the horizontal or vertical edge of the blade is the convolution of the source function (Gaussian) and the aperture function (step function). This is given by $I(x)=1/2(1+erf(x/w))$ where $erf()$ is the error function, and w/M is the 1/e source radius with magnification M. Figure 4 (d,e,f) shows horizontal lineouts of the corresponding images (a,b,c) along with the best fit of the intensity function $I(x)$.

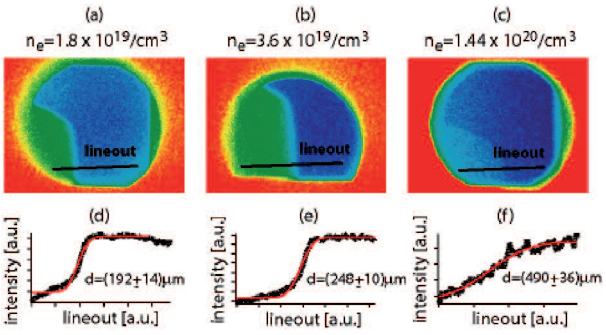

Figure 4. (a,b,c) Penumbral images taken with the edge of a razor blade for different plasma densities. (d,e,f) corresponding horizontal lineouts with best fit to determine the source size.

Knife edge measurements were taken for different electron plasma densities for constant focused intensity $(1.3\pm0.4)\times10^{21}$ Wcm^{-2}. Plotting the full width *1/e* source size in horizontal and vertical direction versus the electron density, one can see the increase of the source size with density (Fig. 5 (left)). Since the imaging plates were filtered with a 22 µm sheet of Al foil, the source size given by the knife edge method is due to x-rays with energies greater than the *1/e* filter energy 5.1 keV.

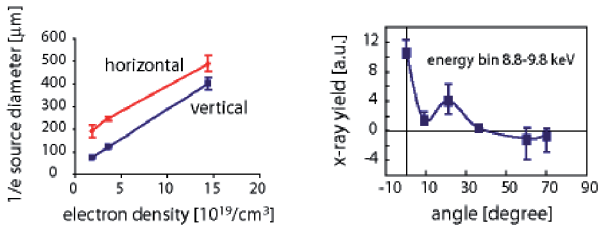

Figure 5. (left) source size diameter as a function of electron density as measured with a pair of orthogonal knife edges. (right) angular distribution of the x-ray signal as measured with the Ross filter detectors for an *fl5* shot with $a_0=13.6$.

Comparing the independent source size measurements obtained with the pinhole and knife edge method, we find that the pinhole camera yields twice the size for both the horizontal and vertical lineouts. This can to be attributed to the lower filtering energy of the pinhole (4.0 keV) compared to the knife edge (5.1keV).

It cannot be taken for granted that the origin of the observed x-ray radiation is the interaction of the high intensity laser field with the electrons and their nonlinear motion. One must also consider other sources, such as accelerated electrons causing bremsstrahlung when they hit the nozzle of the gas jet. Therefore, the brass nozzle was replaced by a low *Z* plastic nozzle which will significantly reduce bremsstrahlung. Since this did not affect the source size measurements, it is clear that bremsstrahlung from the nozzle must be negligible.

In a second series of experiments, an array of 16 Ross filter detectors was set up as depicted in Fig. 2. Ross Filter pairs were equipped with individual magnets of 0.3 T x 5 cm, at distances 56 and 64 cm to deflect electrons with energies up to 71 and 53 MeV respectively by more than 2 cm, in order to miss the Ross filter. Each filter was coupled to a piece of image plate, sitting in a lead housing with a 4 cm long 1 cm diameter lead collimator pointing at the target (refer to inset in Fig. 2). This reduces the chance of picking up undesired background radiation from random directions. Moreover, each lead collar is equipped with two orthogonal wire crosses made from 100 µm and 250 µm copper respectively. These wires are opaque to x-rays with energies lower than 29 keV, whereas they are rather transparent to electrons of energies above 53 MeV, which have a *1/e* stopping distance of greater than 10 mm in copper.[7] Therefore, the shadow of a wire cross projected onto the image plate behind the Ross filter pair is a sign of x-rays and not electrons.

Fig. 6 shows the transmission from filter pairs based on Zn/Cu, which were set up at angles 0°, 9°, 36° and 63° respectively. First of all, it can be seen that most of the Ross filter detectors show multiple shadows of each wire cross (Fig. 6 (0°,9°). These multiple shadows are always accompanied by non-uniform transmission levels. Distinct

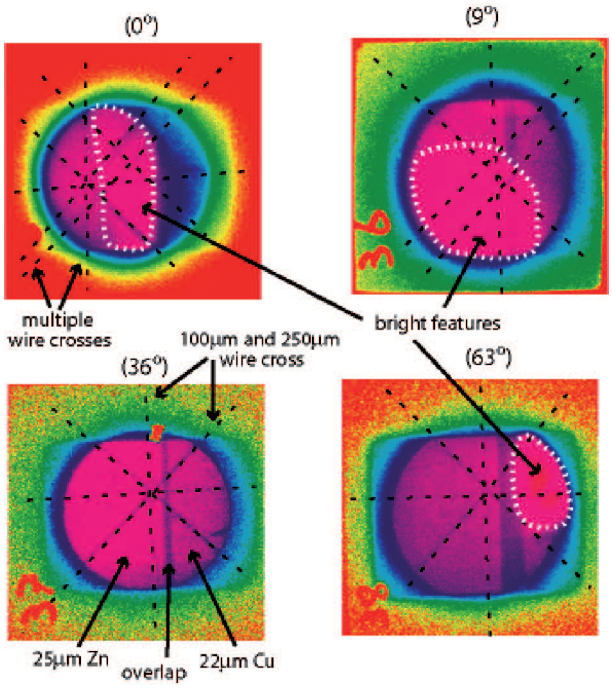

Figure 6. Images taken with a set of Zn/Cu Ross filter detectors, set up from different angles ($n_e=1.4\times10^{20}$cm^{-3}, $I=1.6\times10^{21}$ W/cm^2)

bright features of significant size appear (Fig 6.). These features do not change with laser energy, focusing geometry or gas density, but they do correlate with the setup of the magnets. When magnets are removed, only a single wire shadow was observed. Multiple shadows must be the result of collimated beams of x-rays or particles that enter the lead collar of the Ross detector from different direction. The typical offset between two shadows of the same cross is several mm. This requires the two corresponding sources to be 1-3 cm apart from each other, assuming they were sitting in proximity to the magnets. In fact, one can imagine low energy electrons being deflected by the magnets and stopped inside their mounts, giving rise to a secondary x-ray source. One could also imagine that (low energy) electrons enter the magnets from various angles and are therefore deflected into the lead collar giving rise to additional shadows of the wire crosses.

The present measurements make it difficult to extract reliable angular and spectral emission patterns. Due to the highly nonuniform background (Fig. 6), a determination of transmitted signal levels is arbitrary. Nevertheless, the signal levels were taken for every Ross filter pair, avoiding areas which contain bright features and multiple shadows as much as possible. Figure 5 (right) shows the x-ray yield as a function of the angle for an energy bin from 8.8-9.8 keV. The plotted data corresponds to a normalized vector potential of $a_0=13.6$ (low energy *fl5* shot). Although it is not clear whether the distinct peak at ~20±10° is real or a systematic artifact, it allows for speculations about its origin. Considering the simplest case of free electrons oscillating inside a laser field at relativistic intensity ($a_0>1$), the angular distribution mainly consists of two lobes collimated in the forward direction.[1] The lobes are centered at an angle of $\theta=tan^{-1}(p_t/p_x)\approx2/a_0$, were pt and px are the components of the electron momentum perpendicular and parallel to the laser propagation axis.

For $a_0=13.6$, this angle turns out to be 8.4º, which is just slightly smaller than what we have observed in the experiment (Fig. 5 (right). However, when the focused intensity was increased to a corresponding $a_0=37$, θ did not shift towards smaller angles as predicted theoretically. Further measurements with reduced background level are required to clarify whether the observed peaks are evidence for Thomson lobes.

Conclusions

We report on the first efforts to field a variety of x-ray diagnostics on Petawatt laser interactions with underdense plasmas from a helium gas jet. It was found, that penumbral and pinhole imaging are suitable options to measure the x-ray source size without interfering with other major diagnostics. The sensitivity of the crystal spectrometer employed was too low to obtain spectral measurements. A high sensitivity x-ray spectrometer with broad angular and spectral coverage based on the Ross filter method was designed and employed. Preliminary experiments show, that further precautions are necessary to eliminate systematic x-ray and electronic/ionic background. By replacing the individual magnets with a single large scale magnet (1T × 20 cm) in proximity to the source, one could deflect electrons with energies up to 300 MeV, also avoiding the problem of multiple sources.

The authors acknowledge the assistance of the staff of the Central Laser Facility at the Rutherford Appleton Laboratory.

References

1. K. Ta Phuoc *et al*., *Phys. Rev. Lett.* **91**, 195001 (2003)
2. A. Rousse *et al*., *Phys. Rev. Lett.* **93**, 135005 (2004), K. Ta Phuoc *et al*., *Phys. Plasmas* **12**, 023101 (2005)
3. S. P. D. Mangles *et al*., *Phys. Rev. Lett.* **94**, 245001 (2005)
4. C. D. Gregory *et al*., *RAL Report,* p195-196, (2003-2004)
5. A. E. Siegman, *Lasers*, University Science Book, CA (1986)
6. http://www.schulz-si.com/
7. http://physics.nist.gov/PhysRefData/Star/Text/contents.html